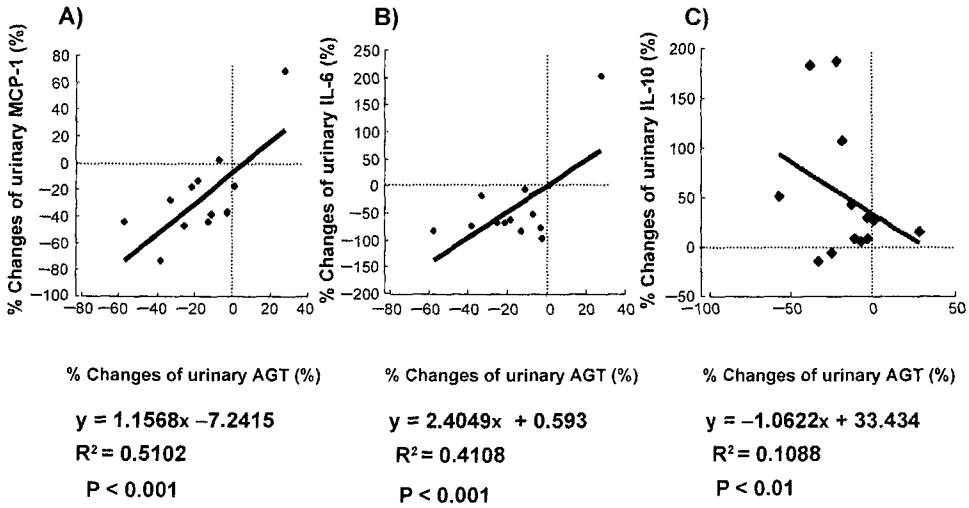

Figure 2. Correlation between the reduction rate of the urinary angiotensinogen (UAGT) levels and those of the monocyte chemoattractant protein (MCP)-1 **A)** interleukin (IL)-6 **B)**, and IL-10 **(C)** levels.

Conclusions

The results of the present study revealed that a vicious cycle of HG-ROS-AGT-Ang II-AT1R-ROS may operate in DN. The continuous increase in the ROS levels contributes to the progression of DN. ARB treatment is believed to suppress ROS production by blocking the Ang II-AT1R-ROS pathway, thus reducing inflammation and suppressing AGT generation.[1-11]

We previously reported that a reduction in the urinary ROS levels is important for ARBs to exert their ACR-lowering effects, and that even with an equal reduction in the blood pressure; ARBs reduce the ROS levels more effectively than other antihypertensive agents.[10] Thus, the action of ARBs in reducing the ROS levels is independent of a decrease in the blood pressure. Accordingly, it seems that the ROS reduction observed in this study may be attributed to the blockade of the Ang II-ROS pathway rather than to decrease in blood pressure. The findings of this study reveal that changes in the UAGT levels largely influence the ARB-induced changes in the ROS levels and ACR. The UAGT levels are reported to be elevated in hypertensive patients and are correlated with the ACR; further, ARB treatment reduces the UAGT levels.[12] Changes in the UAGT levels are correlated with changes in not only the ACR but also the blood pressure; this suggests that AGT in the blood might be filtered in the glomeruli and excreted in urine. Thus, a reduction in the UAGT levels may merely reflect a decrease in the intraglomerular pressure rather than the suppression of AGT production. However, the ARB-induced reduction in the ACR is probably caused by blockade of the ROS-AGT-Ang II-AT1R-ROS cycle. This is because 1) the reduction in the UAGT levels correlated not only with the changes in the ACR and blood pressure but also with the changes in the levels of ROS and inflammatory markers, and 2) AGT is most probably produced in renal cells and released in urine.[1-8] Another possible reason for reduced UAGT excretion may be that ARB increases the renal tubular reabsorption of AGT. Unfortunately, we were unable to investigate this possibility in the present study.

We have previously reported that the efficacy of ARBs increases with urinary oxidative stress.[10] Moreover, we confirmed that the greater the UAGT excretion, the greater is the ACR suppression induced by ARB administration. The fact that the subjects in the present study exhibited increased UAGT and ROS levels indicates that the ROS-AGT-Ang II-AT1R-ROS cycle was strongly activated in these subjects. The stronger the activation of this cycle, the more prominent may be the effects of AT1R blockade. Activation of the AGT-Ang II-ROS pathway increases the intraglomerular pressure and the ACR. Therefore, the RAS-suppressive effects of ARB are believed to

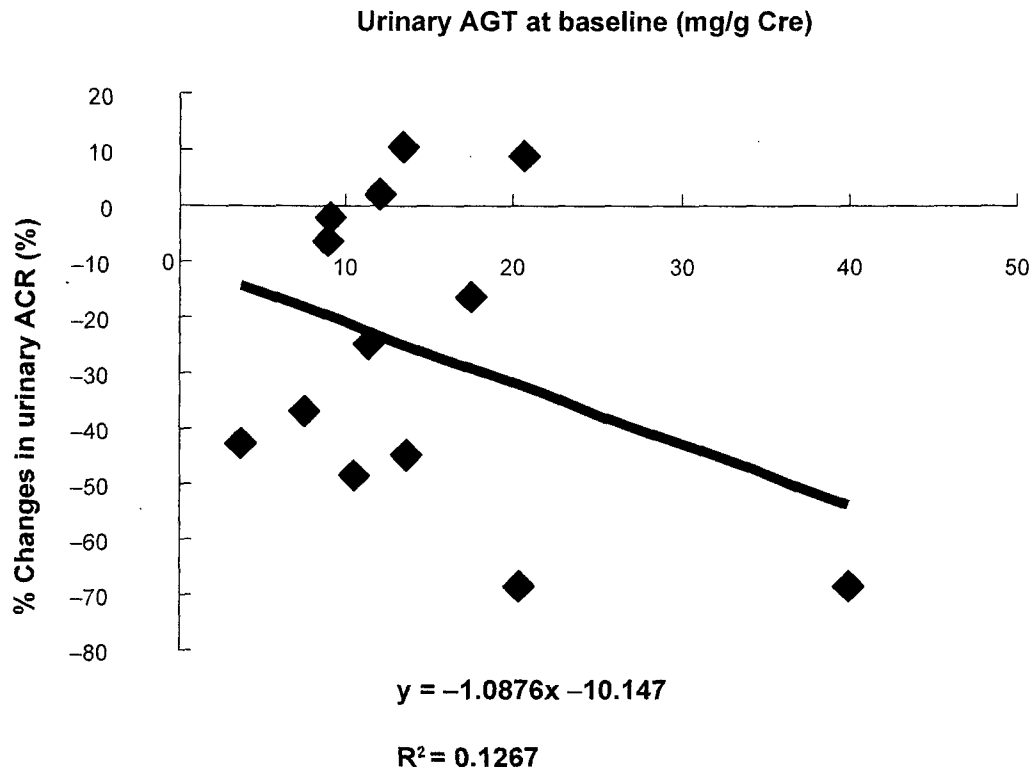

Figure 3. Correlation between the baseline values of urinary angiotensinogen (UAGT) and the reduction rate of urinary albumin excretion (ACR).

increase with UAGT excretion. Considering these implications of ROSs and AGT, we expect that the efficacy of ARBs increases with the UAGT levels.[10] If this is true, UAGT could serve as a predictive factor for the renoprotective effects of ARBs.

The sample size of this study was too small for us to arrive at definitive conclusions; further investigation with a larger sample size is necessary. Furthermore, this study was not a randomized control trial (RCT) comparing ARBs with controls. In addition, since we did not perform examinations like a renal biopsy, we cannot be certain that the DN did in fact improve in our patients. Further clinical research is necessary for clarifying these issues. This research is a preliminary investigation and definitely needs to be followed up with a large-scale RCT. A large-scale RCT of this type, designated as the ORION-ANGEL (Olmesartan Reduces Inflammation and Oxidative stress in Nephropathy and suppresses ANGiotensinogen ELevation) Study (UMIN000001618), is currently underway.

Acknowledgements

This research was supported by grants from the National Institute of Diabetes and Digestive and Kidney Diseases (R01DK072408); the National Center for Research Resources (P20RR017659); and the National Heart, Lung, and Blood Institute (R01HL026371). The authors acknowledge the excellent technical assistance received from Toshie Saito, MD; Akemi Katsurada, MS (Tulane University); Akiko Kubota, MS; Manami Simizu, MS; and Mai Sasaki, MS (Tohoku University).

Disclosure

The authors report no conflicts of interest.

References

1. Vidotti DB, Casarini DE, Cristovam PC, Leite CA, Schor N, Boim MA: High glucose concentration stimulates intracellular renin activity and angiotensin II generation in rat mesangial cells. *Am J Physiol Renal Physiol.* 2004;286:F1039–F45.
2. Yoo TH, Li JJ, Kim JJ, et al. Activation of the renin-angiotensin system within podocytes in diabetes. *Kidney Int.* 2007;71:1019–27.

3. Singh R, Singh AK, Leehey DJ: A novel mechanism for angiotensin II formation in streptozotocin-diabetic rat glomeruli. *Am J Physiol Renal Physiol.* 2005;288:F1183–F90.
4. Hsieh TJ, Zhang SL, Filep JG, Tang SS, Ingelfinger JR, Chan JS: High glucose stimulates angiotensinogen gene expression via reactive oxygen species generation in rat kidney proximal tubular cells. *Endocrinology.* 2002;143:2975–85.
5. Hsieh TJ, Fustier P, Zhang SL, et al. High glucose stimulates angiotensinogen gene expression and cell hypertrophy via activation of the hexosamine biosynthesis pathway in rat kidney proximal tubular cells. *Endocrinology.* 2003;144:4338–49.
6. Zhang SL, Tang SS, Chen X, Filep JG, Ingelfinger JR, Chan JS. High levels of glucose stimulate angiotensinogen gene expression via the P38 mitogen-activated protein kinase pathway in rat kidney proximal tubular cells. *Endocrinology.* 2000;141:4637–46.
7. Brezniceanu ML, Liu F, Wei CC, et al. Catalase overexpression attenuates angiotensinogen expression and apoptosis in diabetic mice. *Kidney Int.* 2007;71:912–23.
8. Brezniceanu ML, Liu F, Wei CC, et al. Attenuation of interstitial fibrosis and tubular apoptosis in db/db transgenic mice overexpressing catalase in renal proximal tubular cells. *Diabetes.* 2008;57:451–9.
9. Wolf G. New insights into the pathophysiology of diabetic nephropathy: from haemodynamics to molecular pathology. *Eur J Clin Invest.* 2004;34: 785–96.
10. Ogawa S, Mori T, Nako K, Kato T, Takeuchi K, Ito S. Angiotensin II type 1 receptor blockers reduce urinary oxidative stress markers in hypertensive diabetic nephropathy. *Hypertension.* 2006;47:699–705.
11. Haugen EN, Croatt AJ, Nath KA. Angiotensin II induces renal oxidant stress in vivo and heme oxygenase-1 in vivo and in vitro. *Kidney Int.* 2000;58:144–52.
12. Kobori H, Alper AB Jr, Shenava R, et al. Urinary angiotensinogen as a novel biomarker of the intrarenal renin-angiotensin system status in hypertensive patients. *Hypertension.* 2009;53:344–50.
13. Katsurada A, Hagiwara Y, Miyashita K, et al. Novel sandwich ELISA for human angiotensinogen. *Am J Physiol Renal Physiol.* 2007;293:F956–F60.
14. Kobori H, Ohashi N, Katsurada A, et al. Urinary angiotensinogen as a potential biomarker of severity of chronic kidney diseases. *J Am Soc Hypertens.* 2008; 2:349–54.

平成２１年度厚生労働科学研究費補助金（循環器疾患等生活習慣病対策総合研究事業）研究分担報告書

糖尿病および代謝疾患への新規の細胞移植治療の開発

研究分担者　齋藤　康　（千葉大学）
研究協力者　武城英明　（千葉大学大学院医学研究院）

研究要旨　メタボリックシンドロームは糖尿病、血管病のハイリスクであることから適切な診断と予防が必要である。しかしながら、糖尿病発症はわが国のみならず世界中で頻度が増加し、高齢化地域では合併症を考慮した基礎インスリン補充の開発も考える必要がある。そこで、糖尿病など代謝疾患を対象に患者脂肪組織由来の初代培養細胞（前脂肪細胞）に補充目的遺伝子を導入しこれを自家移植する普遍的な遺伝子細胞治療法を樹立することを目的に、本研究は、腎不全、視力障害などの合併症を引き越す家族性レシチンコレステロールアシルトランスフェラーゼ（LCAT）欠損症における長期に安定したLCAT補充に関わる新規の治療法の開発に着手した。LCAT遺伝子導入ヒト前脂肪細胞は、GMP製造、移植細胞の品質試験にもとづいて調整した。この細胞が移植後がん化しないことを*in vitro* 及び動物実験で確認した。移植後の持続的LCAT産生とその機能発現解析に必要な薬効評価系及び生着率評価系を確立した。実験動物を用いた移植細胞の生着率の長期検討を実施中である。これらの結果、本研究で用いる前脂肪細胞は、１）形成外科領域で安全に摘出される皮下脂肪組織から比重特性を利用して単離することが可能である、２）レトロウイルスベクターによる遺伝子導入効率が高い、３）形質転換が確認されていない、という優れた特性を有することが明らかになった。病院審査委員会による臨床研究実施計画書の承認を受け厚生労働省へ本計画を申請した。今後、移植細胞の製剤化を行い本治療法の安全性と有効性評価及び生着性を確証することで本治療法の臨床適用を進める予定である。

A．研究目的

糖尿病は日本、米国に加えてアジア地域における多くの人々の生活レベルを規定する疾患である。したがって、そのハイリスクであるメタボリックシンドロームの診断と適切な予防法が重要である。しかしながら、糖尿病を発症した場合、とりわけ高齢者では、合併症を考慮した基礎インスリン補充が求められる。

われわれは、単離・培養及び遺伝子導入の容易さに加えて、特異的に脂肪細胞に分化しがん化などの形質転換の報告がない前脂肪細胞と、分裂細胞への遺伝子導入効率が高く、長期にわたる蛋白質発現が可能な

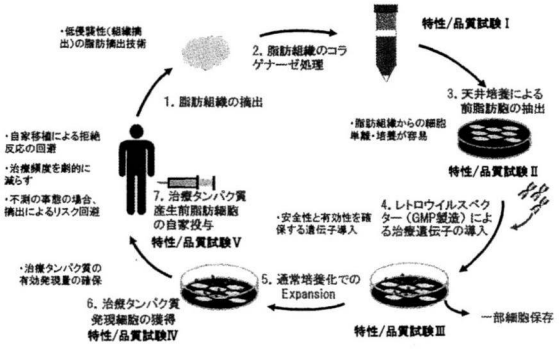

図１　脂肪細胞自己移植による新規の蛋白補充療法

レトロウイルスベクターとの組み合わせに着目し、脂肪細胞移植を用いた新規の蛋白補充技術のコンセプトを糖尿病モデルマウスとヒトインスリン遺伝子導入マウス前脂肪細胞を用いて明らかにした。本研究は、この新規技術を根本的治療法のない家族性LCAT欠損症を対象として臨床応用し新規治療法を実用化することを目的とする。

B & C．研究方法と結果

1．移植細胞の機能評価系の検討

1）LCAT蛋白の検出

B6マウスを用いた移植実験で採取したマウス血及び移植組織を用いhLCATの高感度免疫沈降ウェスタンブロット法(WB)、免疫蛍光染色法を確立した。

2．移植細胞の薬効評価（LCAT蛋白の機能発現評価）

1）LCAT活性測定法

コレステロールを含有する人工リポソームを基質とする高感度測定法を確立した。

2）コレステロールの代謝変化測定

WBを用いたヒト血清リポ蛋白プロファイルの測定法を確立した。

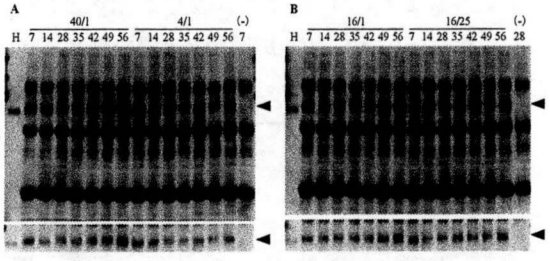

図２　LCAT遺伝子導入脂肪細胞から培養液中に分泌されるLCAT蛋白　H:HDL；Sample:培養上清30 μL；Day 7, 14, 28, 35, 42, 49, 56　フィブリン（mg/mL)/トロンビン（U/mL)；(-)：細胞なし（16/1)；細胞：1x 10^7 cells/mL → 100μL（1x10^6 cells/well）◀:LCAT:LCAT；Exposure：上段 3 min、下段 1 min。

3）前処置による適応能力強化の検討

移植用細胞の分化誘導処理に関しては移植実験の結果、未分化細胞と変化が認められなかった。低酸素・低栄養処理については、細胞の事前処理が細胞のviabilityに悪い影響を与えることが分かった。

4）LCAT欠損マウスでの薬効

リポ蛋白プロファイルにおいてLCAT欠損マウス血清はヒト患者血清と同じ効果が認められず、LCAT欠損マウスは適切なモデル動物ではないと判断した。

5）免疫不全マウスでの生着性及び安全性

フィブリノーゲン 8及び40 mg/mLでLCAT遺伝子導入ヒト前脂肪細胞をNudeマウスに移植し、継続観察中である。

3．　家族性製LCAT欠損症患者を対象とした臨床研究

平成21年7月24日の附属病院遺伝子治療臨床研究審査委員会の承認を受け8月5日に厚生労働大臣官房厚生科学課へ申請書類を提出した。当局からの照会事項に対する回答書を10月21日に提出した。

（倫理面への配慮）

・　移植細胞の薬効薬理および生着性に関する研究は、千葉大学大学院医学研究院の規定に従い、国で定められている、ヒト生体由来細胞を用いた実験、組換え DNA 実験、動物取り扱いに関する指針に従い、千葉大学で開催される各委員会で実験許可を受けて実施した。移植細胞の調製業務は、「遺伝子治療用医薬品の品質及び安全性の確保に関する指針」、「ヒト（自己）由来細胞・組織加工医薬品等の製造管理・品質管理の考え方について」、「医薬品の臨床試験の実施の基準に関する省令」に基づく「治験薬の製造管理及び品質管理基準および治験薬の製造施設の構造設備基準（治験薬 GMP）について」を満たす製造設備及び手順に遵守し製造した。臨床研究の実施に先立ち、臨床研究に関する計画書などについて、千葉大学医学部附属病院遺伝子治療審査委員会において、科学的、倫理的な観点から審議を受け、承認を受け行う。

DおよびE．考察および結論

本研究は、根本的治療法のない家族性LCAT欠損症を対象として、遺伝子導入脂肪細胞の自己移植という新規の補充療法を世界で初めて実用化するトランスレーショナル研究である。家族性LCAT欠損症に対する食事療法及び輸

血によるLCAT補充療法はいずれも効果が不十分であるとともに、遺伝子組換型LCAT製剤の研究開発は行われていない。他の疾患治療法としてアデノウイルスベクターを用いた動物での遺伝子治療法の検討が報告されているが実用化までの課題は多い。

これらの課題を克服できる本治療法の特徴は、すでに形成外科臨床領域で行われている脂肪吸引、脂肪移植を応用して遺伝子導入脂肪細胞を製品化し、自己移植により目的蛋白を長期にわたり安定して補充するという、これまで医療経済的に蛋白補充が困難であったまれな難治性疾患に広く応用することが可能な新規技術であることである。しかしながら、自家移植した前脂肪細胞は、その生存が認められるとはいえ、移植後の減少は避けられず、治療目的に応じた移植条件の至適化検討が求められる。外来遺伝子を導入した移植細胞での治療目的蛋白質の持続的発現は動物及びヒトで一部見られているが、その安定した薬効発現のためには、*in vitro* 及び *in vivo* での多面的検討が必要である。

本研究により、LCAT搭載レトロウイルスベクター及び移植細胞のGMP製造法と品質試験法を確立した。また、*in vitro* 及び動物でのそれらの安全性を確認し、薬効評価系及び生着率評価系を確立した。今後、本治療法の実用化に必須な移植細胞の生着率向上と製剤化の検討が必要である。移植後の持続的なLCAT産生を確保するための、移植細胞の生着率向上を目的とする製剤化検討を行うとともに、臨床研究の実施準備に着手する。これらの基礎検討を実施し十分な安全性配慮と法令等遵守のもと本治療法の安全性並びに有効性評価及び生着性を検証する臨床研究を家族性LCAT欠損症患者を対象に実施する予定である。

F. 健康危険情報

特記事項なし

G. 研究発表

論文発表

1) Matsuo, M, Ebinuma, H, Fukamachi, I, Jiang, M, Bujo, H, Saito, Y. (2009) Development of an immunoassay for the quantification of soluble LR11, a circulating marker of atherosclerosis. *Clin Chem.* 55, 1801-1808.

2) Tashiro, J, Miyazaki, O, Nakamura, Y, Miyazaki, A, Fukamachi, I, Bujo, H, Saito, Y. (2009) Plasma pre beta1-HDL level is elevated in unstable angina pectoris. *Atherosclerosis.* 204, 595-600.

3) Takahashi, M, Bujo, H, Jiang, M, Noike, H, Saito, Y, Shirai K. (2010) Enhanced circulating soluble LR11 in patients with coronary organic stenosis. *Atherosclerosis.* in press.

H. 知的財産権の出願、登録状況

なし

研究成果の刊行に関する一覧表

雑誌

発表者氏名	論文タイトル名	発表誌名	巻号	ページ	出版年
Takahashi M, Bujo H, Jiang M, Noike H, Saito Y, Shirai K.	Enhanced circulating soluble LR11 in patients with coronary organic stenosis.	Atherosclerosis	2009 Dec 16. [Epub ahead of print]		
Matsuo M, Ebinuma H, Fukamachi I, Jiang M, Bujo H, Saito Y.	Development of an immunoassay for the quantification of soluble LR11, a circulating marker of atherosclerosis.	Clin Chem	55(10)	1801-8.	2009
Tashiro J, Miyazaki O, Nakamura Y, Miyazaki A, Fukamachi I, Bujo H, Saito Y.	Plasma pre beta1-HDL level is elevated in unstable angina pectoris.	Atherosclerosis	204(2)	595-600	2009

Atherosclerosis 204 (2009) 595–600

Contents lists available at ScienceDirect

Atherosclerosis

journal homepage: www.elsevier.com/locate/atherosclerosis

Plasma preβ1-HDL level is elevated in unstable angina pectoris

Jun Tashiro[a,c], Osamu Miyazaki[b,*], Yoshitake Nakamura[c], Akira Miyazaki[c], Isamu Fukamachi[b], Hideaki Bujo[d], Yasushi Saito[e]

[a] Department of Internal Medicine, Matsudo City Hospital, 4005, Kamihongo, Matsudo, Chiba 271-8511, Japan
[b] Tsukuba Research Institute, Sekisui Medical Co. Ltd. (Daiichi Pure Chemicals Co. Ltd.), 3-3-1, Koyodai, Ryugasaki, Ibaraki 301-0852, Japan
[c] Department of Cardiology, Chiba Cardiovascular Center, 575, Tsurumai, Ichihara, Chiba 290-0512, Japan
[d] Department of Genome Research and Clinical Application, Chiba University Graduate School of Medicine, 1-8-1, Inohana, Chuo-ku, Chiba 260-8670, Japan
[e] Department of Clinical Cell Biology, Chiba University Graduate School of Medicine, Chiba University, 1-8-1, Inohana, Chuo-ku, Chiba 260-8670, Japan

ARTICLE INFO

Article history:
Received 30 June 2008
Received in revised form 8 October 2008
Accepted 10 October 2008
Available online 1 November 2008

Keywords:
Preβ1-HDL
Acute coronary syndrome
HDL
Reverse cholesterol transport
LCAT

ABSTRACT

Preβ1-HDL, a minor HDL subfraction consisting of apolipoprotein A-I (apoA-I), phospholipids and unesterified cholesterol, plays an important role in reverse cholesterol transport. Plasma preβ1-HDL levels have been reported to be increased in patients with coronary artery disease (CAD) and dyslipidemia. To clarify the clinical significance of measuring plasma preβ1-HDL levels, we examined those levels in 112 patients with CAD, consisting of 76 patients with stable CAD (sCAD) and 36 patients with unstable angina pectoris (uAP), and in 30 patients without CAD as controls. The preβ1-HDL levels were determined by immunoassay using a specific monoclonal antibody (Mab55201) that we established earlier. The mean preβ1-HDL level in the CAD patients was significantly higher than the level in the controls (34.8 ± 12.9 mg/L vs. 26.6 ± 6.9 mg/L, $p < 0.001$). In addition, the mean preβ1-HDL level was markedly higher in the uAP subgroup than in the sCAD subgroup (43.1 ± 11.5 mg/L vs. 30.9 ± 11.7 mg/L, $p < 0.0001$). These tendencies remained even after excluding dyslipidemic subjects.

These results suggest that elevation of the plasma preβ1-HDL level is associated with the atherosclerotic phase of CAD and may be useful for identifying patients with uAP.

1. Introduction

Preβ1-HDL, an HDL subfraction consisting of one or two molecules of apolipoprotein A-I (apoA-I), small amounts of phospholipids and unesterified cholesterol, plays an important role in reverse cholesterol transport, although it comprises only 1–5% of total apoA-I in blood plasma [1–4]. The initial step of reverse cholesterol transport, called cholesterol efflux, is a reaction by which excessively accumulated cholesterol in peripheral tissues is removed by HDL. Preβ1-HDL is known as the initial plasma acceptor of cell-derived cholesterol [1–5].

Three pathways have been suggested as routes by which preβ1-HDL is generated [6–11]. The first is a pathway in which preβ1-HDL is formed when lipid-free apoA-I or lipid-poor apoA-I removes cell-derived, unesterified cholesterol, mediated by ATP-binding cassette transporter A1 (ABCA1) located on cell membranes [6–8]. The second is a pathway in which preβ1-HDL is directly secreted from the liver [9,10], and the third is a pathway in which preβ1-HDL is released from α-migrating HDL during its remodeling [11]. As the catabolic pathway of preβ1-HDL, a lecithin–cholesterol acyltransferase (LCAT)-dependent conversion pathway has been suggested. The unesterified cholesterol on the preβ1-HDL is esterified by LCAT, and the preβ1-HDL removes cellular cholesterols, increases in size and is converted to an α-migrating HDL [12–14].

Thus, preβ1-HDL is proposed to be a key component of reverse cholesterol transport. We previously reported development of a monoclonal antibody (Mab55201) specifically recognizing an epitope of apoA-I that is exposed only in preβ1-HDL, and we established an ELISA system for direct measurement of preβ1-HDL using Mab55201 [15]. The method provides a way to investigate the clinical significance of measuring plasma preβ1-HDL levels.

Plasma preβ1-HDL levels have been reported to be elevated in patients with coronary artery disease (CAD) and dyslipidemia [15–17]. However, the mechanism responsible for elevation of the preβ1-HDL level has not been clarified. In this study we examined whether the preβ1-HDL level is elevated in normolipidemic CAD patients and whether the levels differ between patients with unstable angina pectoris (uAP) and those with stable CAD (sCAD), including stable effort angina pectoris and old myocardial infarction. In addition, we studied the relationship between

* Corresponding author. Tel.: +81 297 62 6425; fax: +81 297 62 8635.
E-mail address: miyazaki084@sekisui.jp (O. Miyazaki).

0021-9150/$ – see front matter © 2008 Elsevier Ireland Ltd. All rights reserved.
doi:10.1016/j.atherosclerosis.2008.10.015

Table 1
Baseline characteristics of the study subjects.

	CAD (n = 112)	p^*	Normolipidemic CAD (n = 37)	p^*	Controls (n = 30)
Age (years)	65.8 ± 9.1	n.s.	65.5 ± 9.0	n.s.	66.3 ± 8.3
BMI (kg/m^2)	24.0 ± 2.7	n.s.	24.1 ± 3.4	n.s.	23.3 ± 2.9
SBP (mmHg)	127 ± 18.8	n.s.	123 ± 19.7	<0.05	134 ± 14.2
DBP (mmHg)	74.1 ± 11.7	n.s.	71.7 ± 12.5	<0.05	77.9 ± 9.7
HbA1c (%)	7.3 ± 1.4	<0.05	7.1 ± 1.4	n.s.	6.4 ± 1.2
T-Cho (mg/dL)	203 ± 41.4	n.s.	181 ± 22.9	n.s.	193 ± 20.3
TG (mg/dL)	142 ± 77.9	<0.001	92.2 ± 25.4	n.s.	85.3 ± 29.3
LDL-C (mg/dL)	131 ± 34.7	0.051	110 ± 21.7	n.s.	115 ± 16.1
HDL-C (mg/dL)	43.9 ± 9.4	<0.0001	49.8 ± 8.6	<0.05	55.2 ± 11.2
ApoA-I (mg/dL)	115 ± 18.5	<0.0001	123 ± 16.6	<0.01	137 ± 21.0
ApoB (mg/dL)	108 ± 27.3	<0.01	90.0 ± 16.1	n.s.	93.4 ± 12.3
Creatinine (mg/dL)	0.93 ± 0.32	<0.01	0.93 ± 0.34	<0.01	0.73 ± 0.18
BUN (mg/dL)	17.7 ± 7.3	n.s.	16.8 ± 4.0	n.s.	15.4 ± 4.0
AST (IU/L)	37 ± 19.5	n.s.	38.1 ± 16.3	n.s.	32.0 ± 11.0
ALT (IU/L)	27.4 ± 20.2	<0.05	29.1 ± 22.8	<0.05	19.0 ± 9.0
ChE (U/L)	325 ± 77.6	n.s.	308 ± 77.9	n.s.	316 ± 67.2
Medications, n (%)					
Aspirin	90 (80.4%)	<0.0001	28 (75.7%)	<0.0001	2 (6.7%)
Nitrates	87 (77.7%)	<0.0001	24 (64.9%)	<0.0001	1 (3.3%)
Calcium channel blockers	51 (45.5%)	n.s.	17 (45.9%)	n.s.	13 (43.3)
Beta blockers	37 (33.0%)	n.s.	10 (27.0%)	n.s.	5 (16.7%)
ACE inhibitors	26 (23.2%)	n.s.	8 (21.6%)	n.s.	3 (10.0%)
Diuretics	10 (8.9%)	n.s.	3 (8.1%)	n.s.	1 (3.3%)
Digoxin	6 (5.4%)	n.s.	0 (0.0%)	n.s.	1 (3.3%)
ARBs	2 (1.8%)	n.s.	1 (2.7%)	n.s.	1 (3.3%)
Antiplatelet	27 (24.1%)	<0.01	9 (24.3%)	<0.01	0 (0.0%)
Antidiabetics	45 (40.2%)	n.s.	13 (35.1%)	n.s.	9 (30.0%)
Lipid-lowering agents	3 (2.7%)	n.s.	1 (2.7%)	n.s.	0 (0.0%)

Data are shown as mean ± S.D. or number. ARBs: angiotensin II receptor blockers.
* Significance vs. controls.

the preβ1-HDL level and lipid metabolism by examining for correlations between the preβ1-HDL level and the concentrations or activities of various lipid metabolic markers.

2. Methods

2.1. Study subjects

One hundred and twelve coronary artery disease patients were recruited from inpatients and outpatients of Chiba Cardiovascular Center (Chiba, Japan). The diagnosis of CAD was based on a history of myocardial infarction, clinical symptoms including prolonged chest pain, and the presence of angiographically demonstrated stenosis (≥75% obstructive lesions). The CAD group was divided into 36 patients with uAP and 76 patients with sCAD based on the clinical symptoms. uAP was diagnosed in accordance with the American Heart Association (AHA) classification (1975): the presence of chest pain which began during the previous 3 weeks and most recently occurred within the previous 1 week; and the absence of both ST segment elevation on the electrocardiogram and serum biochemical markers of cardiac necrosis. All patients with uAP belonged to class I or II in severity and class B or C in the clinical circumstances according to Braunwald's classification (1989). The sCAD subgroup was composed of 32 patients with stable effort angina pectoris and 44 patients with old myocardial infarction. We also enrolled 30 age- and BMI-matched subjects as the control group. The control subjects were recruited from outpatients of Chiba Cardiovascular Center and included type 2 diabetics and/or hypertension patients without dyslipidemia and no history of CAD. The control subjects were all confirmed to have no cardiac disorders on the exercise-loaded electrocardiogram. Normolipidemic subjects in the CAD group and the control group were determined on the basis of the concentrations of four serum lipid markers, i.e., total cholesterol (T-Cho) <220 mg/dL, LDL-cholesterol (LDL-C) <140 mg/dL, triglyceride (TG) <150 mg/dL, and HDL-cholesterol (HDL-C) ≥40 mg/dL. Patients with renal and/or liver dysfunction were excluded from this study.

We obtained informed consent from all participants at entry. This study was conducted in accordance with the Declaration of Helsinki of the World Medical Association.

2.2. Blood collection

Venous blood samples for plasma and serum were drawn from the subjects after fasting for one night. The blood samples for plasma were drawn into plastic tubes containing EDTA-2Na, immediately chilled in ice water and centrifuged at 2 °C. The plasma was diluted with 20 volumes of 50% sucrose solution for stabilization and then stored at −80 °C until preβ1-HDL was assayed. The blood samples for serum were separated and stored at −80 °C until assay for serum lipids, apolipoproteins, LCAT activity and other markers of liver or renal function.

2.3. Measurement of preβ1-HDL and biochemical parameters

Preβ1-HDL levels were measured by a sandwich enzyme immunoassay using Mab55201 [15,18]. The preβ1-HDL level was expressed as both an absolute value and a relative value. The absolute value indicates the preβ1-HDL concentration (mg/L) in the plasma, and the relative value indicates the percentage of preβ1-HDL in the total apolipoprotein A-I in the plasma.

The T-Cho, TG, LDL-C, HDL-C, creatinine, blood urea nitrogen (BUN), aspartate transaminase (AST), alanine transaminase (ALT) and cholinesterase (ChE) concentrations were determined enzymatically using an automated analyzer. Apolipoprotein concentrations were determined by immunoturbitometry with commercial reagents from Daiichi Pure Chemicals (Tokyo, Japan), using an automated analyzer. Hemoglobin A1c (HbA1c) was determined by an automated liquid-chromatographic system. LCAT

Table 2
Comparisons of preβ1-HDL levels between CAD and control groups and between uAP and sCAD subgroups.

	n	Preβ1-HDL (mg/L)	p	Preβ1-HDL/apoA-I (%)	p
CAD	112	34.8 ± 12.9	<0.001*	3.05 ± 1.04	<0.0001*
Normolipidemic CAD	37	36.2 ± 12.8	<0.001*	2.94 ± 0.95	<0.0001*
CAD (HDL-C ≥ 40 mg/dL)	74	36.9 ± 13.1	<0.0001*	2.98 ± 0.97	<0.0001*
CAD (high LCAT**)	28	36.5 ± 12.3	<0.001*	3.15 ± 0.93	<0.0001*
Controls	30	26.6 ± 6.9	-	1.97 ± 0.51	-
uAP	36	43.1 ± 11.5	<0.0001	3.66 ± 0.95	<0.0001
sCAD	76	30.9 ± 11.7		2.76 ± 0.95	
Normolipidemic					
uAP	16	43.1 ± 9.1	<0.01	3.42 ± 0.76	<0.01
sCAD	21	30.9 ± 12.8		2.58 ± 0.94	
HDL-C ≥ 40 mg/dL					
uAP	26	44.9 ± 11.6	<0.0001	3.54 ± 0.87	<0.001
sCAD	48	32.6 ± 11.9		2.68 ± 0.89	
HDL-C < 40 mg/dL					
uAP	10	38.3 ± 10.3	<0.05	4.00 ± 1.10	<0.01
sCAD	28	28.1 ± 11.0		2.90 ± 1.05	

Data are shown as mean ± S.D.
* Significance vs. controls.
** LCAT activity ≥80 nmol/mL/h/37 °C.

activities were determined only in 58 randomly selected CAD (9 uAP and 49 sCAD) patients, by the method of Nagasaki and Akanuma using an endogenous substrate [19].

2.4. Statistics

Statistical analyses were performed using Stat Flex for Windows ver. 5.0 (Artech Inc., Osaka, Japan). The difference between two groups was assessed using Student's paired *t*-test. Categorical variables were compared using the χ^2-test. The relationship between two parameters was examined using Pearson's Correlation Coefficient. Receiver-operating characteristic (ROC) curves were plotted, and the area under the curve (AUC) was analyzed to compare the predictive powers of preβ1-HDL, HDL-C and LDL-C for uAP using the sCAD and the control group as reference groups. The AUC indicates the diagnostic accuracy of tests [20]. For all analyses, $p < 0.05$ was considered statistically significant.

Table 3
Comparisons of baseline characteristics between sCAD and uAP subgroups.

	uAP (*n* = 36)	sCAD (*n* = 76)	p
Age (years)	67.0 ± 8.8	65.3 ± 9.2	n.s.
BMI (kg/m²)	24.6 ± 3.4	23.8 ± 2.4	n.s.
SBP (mmHg)	129 ± 22.3	126 ± 16.9	n.s.
DBP (mmHg)	76.8 ± 13.5	72.9 ± 10.7	n.s.
HbA1c (%)	7.5 ± 1.3	7.3 ± 1.4	n.s.
T-Cho (mg/dL)	191 ± 41.8	209 ± 40.2	<0.05
TG (mg/dL)	129 ± 67.4	147 ± 82.1	n.s.
LDL-C (mg/dL)	118 ± 35.6	132 ± 33.5	<0.05
HDL-C (mg/dL)	44.4 ± 9.8	43.6 ± 9.2	n.s.
ApoA-I (mg/dL)	119 ± 20.3	112 ± 17.3	n.s.
ApoB (mg/dL)	100 ± 26.3	112 ± 27.0	<0.05
Creatinine (mg/dL)	0.96 ± 0.29	0.91 ± 0.34	n.s.
BUN (mg/dL)	17.7 ± 4.8	17.8 ± 8.2	n.s.
AST (IU/L)	39.8 ± 21.2	35.7 ± 18.7	n.s.
ALT (IU/L)	28.6 ± 20.6	26.9 ± 20.1	n.s.
ChE (U/L)	30.5 ± 89.8	335 ± 69.6	n.s.
LCAT activity (nmol/mL/h/37 °C)*	72.9 ± 21.0	72.9 ± 12.4	n.s.
Medications, n (%)			
Aspirin	28 (77.8%)	62 (81.6%)	n.s.
Nitrates	27 (75.0%)	60 (78.9%)	n.s.
Calcium channel blockers	16 (44.4%)	35 (46.1%)	n.s.
Beta blockers	12 (33.3%)	25 (32.9%)	n.s.
ACE inhibitors	10 (27.8%)	16 (21.1%)	n.s.
Diuretics	4 (11.1%)	6 (7.9%)	n.s.
Digoxin	1 (2.8%)	5 (6.6%)	n.s.
ARBs	0 (0.0%)	2 (2.6%)	n.s.
Antiplatelet	11 (30.6%)	16 (21.1%)	n.s.
Antidiabetics	9 (25.0%)	36 (47.4%)	<0.05
Lipid-lowering agents	1 (2.8%)	2 (2.6%)	n.s.

Data are shown as mean ± S.D. or number (%). ARBs: angiotensin II receptor blockers.
* Determined in 9 uAP and 49 sCAD patients.

3. Results

3.1. Comparison between CAD patients and controls

Table 1 shows the baseline characteristics of the study subjects. Age, BMI and blood pressure were comparable between the CAD and control groups. The concentrations of HbA1c, TG and apoB were significantly higher, and the concentrations of HDL-C and apoA-I were significantly lower, in the CAD group than in the control group. In the normolipidemic subjects, the only differences were that the concentrations of HDL-C and apoA-I were slightly higher in the control group. Medications were comparable between the CAD and control groups except for aspirin, nitrates and antiplatelet drugs. The absolute and relative values for the preβ1-HDL level were markedly higher in the CAD group than in the control group. These differences were also seen even in the normolipidemic subjects only (Table 2). We then compared the preβ1-HDL levels between the CAD subgroups with high HDL-C (≥40 mg/dL) or high LCAT activity (≥80 nmol/mL/h/37 °C) and the control group. The preβ1-HDL levels were markedly higher in both the CAD subgroups than in the control group (Table 2).

3.2. Comparison between uAP and sCAD subgroups

We divided the CAD group into a uAP subgroup and an sCAD subgroup and compared the preβ1-HDL levels between them. The absolute and relative values for the preβ1-HDL level were markedly higher in the uAP subgroup than in the sCAD subgroup. Moreover, even in the comparisons using only the normolipidemic subjects, only the high HDL-C (≥40 mg/dL) subjects and only the low HDL-C (<40 mg/dL) subjects, the differences remained significant between the two subgroups (Table 2). On the other hand, the concentrations of lipid markers, age, BMI, blood pressure, renal and hepatic function markers and medications did not differ between the uAP and

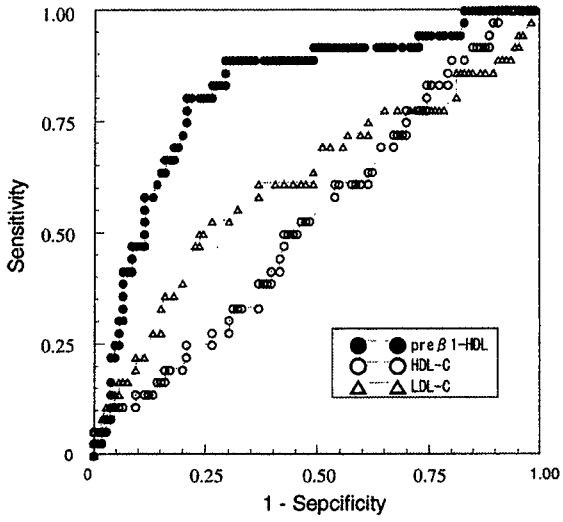

Fig. 1. ROC curves of preβ1-HDL, HDL-C, LDL-C for diagnosis of uAP. The true-positive rate (sensitivity as *y* axis) was plotted vs. the false-positive rate (1-specificity as *x* axis) by changing the cutoff values for the test. The areas under the curves were 0.821 (95% CI, 0.780–0.863) for preβ1-HDL, 0.536 (95% CI, 0.482–0.591) for HDL-C and 0.616 (95% CI, 0.557–0.675).

Table 4
Correlations between preβ1-HDL and clinical factors.

	CAD group (n = 112)		Control group (n = 30)	
	r	p	r	p
Age	0.163	n.s.	−0.122	n.s.
BMI	0.134	n.s.	−0.026	n.s.
SBP	−0.037	n.s.	0.117	n.s.
DBP	0.003	n.s.	0.115	n.s.
HbA1c	0.127	n.s.	−0.039	n.s.
T-Cho	0.146	n.s.	−0.013	n.s.
TG	0.200	<0.05	−0.157	n.s.
LDL-C	0.025	n.s.	−0.054	n.s.
HDL-C	0.247	<0.01	0.194	n.s.
ApoA-I	0.400	<0.0001	0.189	n.s.
ApoB	0.070	n.s.	−0.157	n.s.
Creatinine	0.172	n.s.	−0.012	n.s.
BUN	0.183	n.s.	0.181	n.s.
AST	0.182	n.s.	0.035	n.s.
ALT	0.207	<0.05	−0.195	n.s.
ChE	0.068	n.s.	−0.033	n.s.
LCAT activity*	0.204	n.s.	–	–

* Determined in 58 CAD patients.

sCAD subgroups, except that the concentrations of T-Cho, LDL-C and apoB were slightly lower and that the patients taking antidiabetics were slightly fewer in number in the uAP subgroup (Table 3).

3.3. Preβ1-HDL as a diagnostic marker of uAP

ROC analyses were performed to evaluate preβ1-HDL as a diagnostic marker of uAP. The AUC of preβ1-HDL was significantly greater than that of either HDL-C or LDL-C (vs. HDL-C, $p < 0.0001$; vs. LDL-C, $p < 0.01$) (Fig. 1).

3.4. Correlations between preβ1-HDL level and clinical factors

We examined for correlations between the absolute preβ1-HDL concentration and various clinical factors in the CAD patients and in the control subjects. In the CAD patients, the preβ1-HDL concentration showed a strong, significant positive correlation with apoA-I and a significant positive correlation with HDL-C. On the other hand, no correlation was found with the LDL-C, T-Cho or LCAT activity. TG showed a slightly positive correlation with preβ1-HDL. The only other marker correlating significantly with preβ1-HDL was ALT, which correlated slightly. In the control subjects, none of the factors showed a significant correlation with preβ1-HDL (Table 4).

We then examined for correlations between the preβ1-HDL and the HDL-C, apoA-I or LCAT activity in the uAP and sCAD subgroups separately. HDL-C showed a significant positive correlation with preβ1-HDL in the sCAD subgroup, but not in the uAP subgroup (Fig. 2A). ApoA-I showed a significant positive correlation with preβ1-HDL in both the uAP and sCAD subgroups (Fig. 2B), whereas LCAT activity did not (Fig. 2C).

4. Discussion

The present study clearly showed that the plasma preβ1-HDL level was high in the CAD group even when excluding dyslipidemic patients (Table 2). Earlier studies reported the plasma preβ1-HDL concentration to be elevated in patients with CAD, dyslipidemia and obesity, and also in hemodialysis patients [15–17,21,22]. The present study excluded patients with renal disorders, including hemodialysis patients, and BMI-matched control subjects were

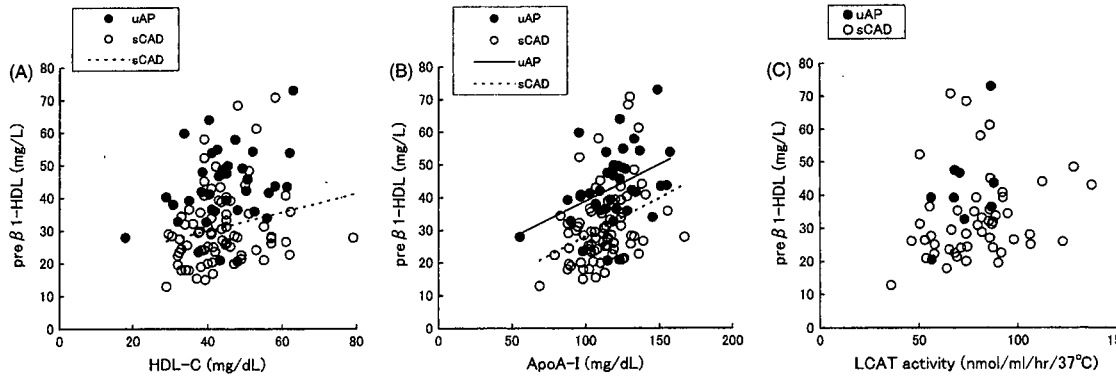

Fig. 2. Correlations (Pearson's Coefficients) between preβ1-HDL levels and HDL-C levels (A), apoA-I levels (B) and LCAT activities (C) in uAP and sCAD subgroups. A: uAP (n = 36), r = 0.313, p = 0.063; sCAD (n = 76), r = 0.227, $p < 0.05$. B: uAP (n = 36), r = 0.394, $p < 0.05$; sCAD (n = 76), r = 0.350, $p < 0.01$. C: uAP (n = 9), r = 0.538, p = 0.135; sCAD (n = 49), r = 0.215, p = 0.139.

used to exclude any effect of obesity. When the CAD group was divided into uAP and sCAD subgroups, the preβ1-HDL level was markedly higher in the uAP subgroup than in the sCAD subgroup. Moreover, the difference remained significant even when dyslipidemic patients were excluded from the two subgroups (Table 2). The age, BMI, blood pressure and concentrations of HbA1c, hepatic function markers, renal function markers, HDL-C and apoA-I did not differ significantly between the two subgroups, although T-Cho, LDL-C and apoB were somewhat lower in the uAP subgroup than in the sCAD subgroup (Table 3). ROC analyses were performed to investigate the potential of preβ1-HDL as a predictive marker for uAP. Preβ1-HDL showed better diagnostic accuracy than other lipid markers, suggesting that preβ1-HDL may be useful for identifying patients with uAP (Fig. 1).

Two earlier studies reported elevation of the preβ1-HDL levels in CAD patients [16,17]. However, the mechanism responsible for that elevation has not been elucidated. Miida et al. reported that delayed catabolism of preβ1-HDL, specifically, delayed LCAT-dependent conversion of preβ1-HDL into α-migrating HDL, causes elevation of the preβ1-HDL level in CAD patients. However, they also described that some CAD patients had a high preβ1-HDL level despite the high LCAT activity, suggesting that some other mechanism may be responsible for preβ1-HDL elevation [16]. Asztalos et al. reported that CAD patients with low HDL-C levels (≤35 mg/dL) have high preβ1-HDL levels and suggested that delayed catabolism of preβ1-HDL is responsible for the elevated preβ1-HDL [17]. In our study, the normolipidemic CAD patients, excluding those with low HDL-C levels (<40 mg/dL), also showed elevated preβ1-HDL levels (Table 2). We speculate that the many uAP patients included in the present study may have been the cause of the elevated preβ1-HDL level in CAD patients without dyslipidemia. If, as has been suggested [17], delayed catabolism of preβ1-HDL is responsible for preβ1-HDL elevation, the HDL-C concentration and LCAT activity should be lower in the uAP subgroup than in the sCAD subgroup and should correlate negatively with the preβ1-HDL concentration. However, we could not find any difference in either the HDL-C concentration or the LCAT activity between the uAP and sCAD subgroups (Table 3), and there was no negative correlation between the preβ1-HDL concentration and either the HDL-C concentration or the LCAT activity in the CAD patients. In fact, the preβ1-HDL concentration conversely showed a significant and positive correlation with the HDL-C concentration in the CAD patients (Table 4 and Fig. 2A). In addition, the CAD patients with either a high HDL-C level or high LCAT activity also showed an elevated preβ1-HDL level (Table 2). These results suggest that some other mechanism must be responsible for preβ1-HDL elevation.

Perhaps that mechanism is enhancement of preβ1-HDL formation. The following three formation pathways are known: synthesis in the liver [9,10], new formation through interaction of apoA-I and peripheral cells [6–8] and dissociation through remodeling of α-HDL [11]. In the case of CAD, the last two of these preβ1-HDL formation pathways seem most likely and are discussed below.

Preβ1-HDL formation is increased in atherosclerotic CAD due to accelerated interaction of apoA-I and peripheral cells. It was reported that foam cell formation enhanced expression of ATP-binding cassette transporter A1 and apoA-I-mediated cholesterol efflux from cells in *in vitro* experiments [23,24]. Since preβ1-HDL is formed by the cellular cholesterol efflux of lipid-free apoA-I or lipid-poor apoA-I mediated by ABCA1 [3,4,6–8], the formation of preβ1-HDL in atherosclerotic CAD caused by accumulation of excess cholesterol might be accelerated by enhancement of that efflux in the peripheral cells.

The other most likely pathway of preβ1-HDL formation in uAP is that preβ1-HDL generation is enhanced by α-HDL remodeling caused by an increase in acute-phase proteins during inflammation. Serum amyloid A (SAA), group IIa secretory phospholipase A2 (sPLA2-IIa) and phospholipid transfer protein (PLTP), whose blood concentrations or activities are elevated in the acute-phase, are known to be factors that facilitate α-HDL remodeling [25–28]. For example, it was reported that the amount of SAA in HDL particles increases markedly during the acute inflammatory phase [28] and that it dissociates preβ1-HDL from α-HDL when it binds to α-HDL [29]. The blood concentration of SAA increases in uAP [30], and SAA is highly expressed in atherosclerotic lesions [31]. van der Westhuyzen et al. suggested a model for the acute-phase response in CAD in which SAA and sPLA2-IIa, present at sites of inflammation and tissue damage, play protective roles by enhancing cellular cholesterol efflux, thereby promoting the removal of excess cholesterol from macrophages [25]. Thus, acute-phase proteins, including SAA, seem to be factors promoting preβ1-HDL elevation in uAP, although the results of the present study are not sufficient to prove this hypothesis.

In summary, we demonstrated that the preβ1-HDL level is elevated in CAD patients, especially in uAP patients, even when excluding dyslipidemic subjects. These results suggest that elevation of the plasma preβ1-HDL level is associated with the atherosclerotic phase of CAD. Elevation of plasma preβ1-HDL may be useful for the identification of patients with uAP. Moreover, that elevation may be caused by a different mechanism from the previously proposed delayed catabolism of preβ1-HDL due to low LCAT activity.

Acknowledgement

We wish to thank Isao Nishina of Chiba Cardiovascular Center for his fine technical assistance.

References

[1] Castro GR, Fielding CJ. Early incorporation of cell-derived cholesterol into pre-β-migrating high-density lipoprotein. Biochemistry 1988;27:25–9.
[2] Barrans A, Jaspard B, Barbaras R, et al. Pre-β HDL: structure and metabolism. Biochim Biophys Acta 1996;1300:73–85.
[3] Fielding CJ, Fielding PE. Molecular physiology of reverse cholesterol transport. J Lipid Res 1995;36:211–28.
[4] Sviridov D, Nestel P. Dynamics of reverse cholesterol transport: protection against atherosclerosis. Atherosclerosis 2002;161:245–54.
[5] Yokoyama S. Apolipoprotein-mediated cellular cholesterol efflux. Biochim Biophys Acta 1998;1392:1–15.
[6] Okuhira K, Tsujita M, Yamauchi Y, et al. Potential involvement of dissociated apoA-1 in the ABCA1-dependent cellular lipid release by HDL. J Lipid Res 2004;45:645–52.
[7] Fitzgerald ML, Morris AL, Chroni A, et al. ABCA1 and amphipathic apolipoproteins form high-affinity molecular complexes required for cholesterol efflux. J Lipid Res 2004;45:287–94.
[8] Chau P, Nakamura Y, Fielding CJ, et al. Mechanism of prebeta-HDL formation and activation. Biochemistry 2006;45:3981–7.
[9] Jones LA, Teramoto T, John DJ, et al. Characterization of lipoproteins produced by the perfused rhesus monkey liver. J Lipid Res 1984;25:319–35.
[10] Castle CK, Pape ME, Marotti KR, et al. Secretion of pre-beta-migrating apoA-I by cynomolgus monkey hepatocytes in culture. J Lipid Res 1991;32:439–47.
[11] Rye KA, Clay MA, Barter PJ. Remodeling of high density lipoproteins by plasma factors. Atherosclerosis 1999;145:227–38.
[12] Glomset JA. The lecithin:cholesterol acyltransferase reaction. J Lipid Res 1968;9:155–67.
[13] Francone OL, Gurakar A, Fielding C. Distribution and functions of lecithin:cholesterol acyltransferase and cholesteryl ester transfer protein in plasma lipoproteins. J Biol Chem 1989;264:7066–72.
[14] Nakamura Y, Kotite L, Gan Y, et al. Molecular mechanism of reverse cholesterol transport: reaction of pre-β-migrating high-density lipoprotein with plasma lecithin/cholesterol acyltransferase. Biochemistry 2004;43:14811–20.
[15] Miyazaki O, Kobayashi J, Fukamachi I, et al. A new sandwich enzyme immunoassay for measurement of plasma pre-β1-HDL levels. J Lipid Res 2000;41:2083–8.
[16] Miida T, Nakamura Y, Inano K, et al. Preβ1-high density lipoprotein increases in coronary artery disease. Clin Chem 1996;42:1992–5.
[17] Asztalos BF, Roheim PS, Milani RL, et al. Distribution of apoA-I-containing HDL subpopulations in patients with coronary heart disease. Arterioscler Thromb Vasc Biol 2000;20:2670–6.

[18] Miida T, Miyazaki O, Nakamura Y, et al. Analytical performance of a sandwich enzyme immunoassay for preβ1-HDL in stabilized plasma. J Lipid Res 2003;44:645–50.
[19] Nagasaki T, Akanuma Y. A new colorimetric method for the determination of plasma lecithin–cholesterol acyltransferase activity. Clin Chim Acta 1977;75:371–5.
[20] Hanley JA, McNeil BJ. A method of comparing the areas under receiver operating characteristic curves derived from the same cases. Radiology 1983;148:839–43.
[21] Sasahara T, Yamashita T, Sviridov D, et al. Altered properties of high density lipoprotein subfractions in obese subjects. J Lipid Res 1997;38:600–11.
[22] Miida T, Miyazaki O, Hanyu O, et al. LCAT-dependent conversion of preβ1-HDL into α-migrating HDL is severely delayed in hemodialysis patients. J Am Soc Nephrol 2003;14:732–8.
[23] Langmann TJ, Klucken M, Reil G, et al. Molecular cloning of the human ATP-binding cassette transport 1 (hABC1): evidence of sterol-dependent regulation in macrophages. Biochem Biophys Res Commun 1999;257:29–33.
[24] Lawn RM, Wade DP, Garbin MR, et al. The Tangier disease gene product ABC1 controls the cellular apolipoprotein-mediated lipid removal pathway. J Clin Invest 1999;104:R25–31.
[25] van der Westhuyzen DR, de Beer FC, Webb NR. HDL cholesterol transport during inflammation. Curr Opin Lipidol 2007;18:147–51.
[26] Tiege UJ, Maugeais C, Cain W, et al. Overexpression of secretory phospholipase A(2) causes rapid catabolism and altered tissue uptake of high density lipoprotein cholesteryl ester and apolipoprotein A-I. J Biol Chem 2000;275:10077–84.
[27] Pussinen PJ, Malle E, Metso J, et al. Acute-phase HDL in phospholipid transfer protein (PLTP)-mediated HDL conversion. Atherosclerosis 2001;155:297–305.
[28] Malle E, Steinmetz A, Raynes JG. Serum amyloid A (SAA): an acute phase protein and apolipoprotein. Atherosclerosis 1993;102:131–46.
[29] Miida T, Yamada T, Yamadera T, et al. Serum amyloid A protein generates preβ1 high-density lipoprotein from α-migrating high density lipoprotein. Biochemistry 1999;38:16958–62.
[30] Kosuge M, Ebina T, Ishikawa T, et al. Serum amyloid A is a better predictor of clinical outcomes than C-reactive protein in non-ST-segment elevation acute coronary syndromes. Circ J 2007;71:186–90.
[31] Meek RL, Urieli-Shoval S, Benditt EP. Expression of apolipoprotein serum amyloid A mRNA in human atherosclerotic lesions and cultured vascular cells: implications for serum amyloid A function. Proc Natl Acad Sci U S A 1994;91:3186–90.

Clinical Chemistry 55:10
1801–1808 (2009)

Development of an Immunoassay for the Quantification of Soluble LR11, a Circulating Marker of Atherosclerosis

Masanao Matsuo,[1] Hiroyuki Ebinuma,[1*] Isamu Fukamachi,[1] Meizi Jiang,[2] Hideaki Bujo,[2] and Yasushi Saito[3]

BACKGROUND: Vascular smooth muscle cells (SMCs) migrate from the arterial media to the intima in the progression of atherosclerosis, and dysfunction of SMCs leads to enhanced atherogenesis. A soluble form of the LDL receptor relative with 11 ligand-binding repeats (sLR11) is produced by the intimal SMCs, and the circulating concentrations of sLR11 likely reflect the pathophysiological condition of intimal SMCs. Furthermore, polymorphism of the LR11 gene has been found to be related to the onset of Alzheimer disease. This study describes the development of a sandwich immunoassay for quantifying sLR11 in human serum and cerebrospinal fluid.

METHODS: We used synthetic peptides or DNA immunization to produce monoclonal antibodies (MAbs) A2-2–3, M3, and R14 against different epitopes of LR11.

RESULTS: sLR11 was immunologically identified as a 250-kDa protein in human serum and cerebrospinal fluid by SDS-PAGE separation, and was purified from serum by use of a receptor-associated protein and MAb M3. An immunoassay for quantification of sLR11 with a working range of 0.25–4.0 μg/L was developed using the combination of MAbs M3 and R14. Treatment of serum with 5.25% n-nonanoyl-N-methyl-d-glucamine reduced the matrix effects of serum on the absorbance detection in the ELISA system. The linear dynamic range of the ELISA spanned the variation of circulating sLR11 concentrations in individuals with atherosclerosis.

CONCLUSIONS: A sandwich ELISA was established for quantifying sLR11 in serum and cerebrospinal fluid. This technique provides a novel means for assessing the pathophysiology of atherosclerosis, and possibly neurodegenerative diseases.

The LDL receptor relative with 11 ligand-binding repeats (LR11)[4] (also known as SorLA) *(1, 2)* is a member of the LDL receptor family and is highly expressed in atheromatous plaques, particularly in the intimal smooth muscle cells (SMCs) at the border between the arterial intima and the media *(3)*. Overproduction of LR11 protein promotes the enhanced migration of SMCs via the upregulation of urokinase-type plasminogen activator receptor *(4, 5)*. LR11 plays an essential role in the angiotensin II–induced mobility of SMCs, and angiotensin II type 1 receptor blockers have been found to reduce intimal thickness through the inhibition of the LR11/urokinase-type plasminogen activator receptor–mediated pathway of intimal SMCs in cuff-injured mice *(6)*. The extracellular domain of the membrane-spanning LR11 is released to yield an active soluble form of LR11 (sLR11) *(5, 7, 8)*. Recombinant sLR11 stabilizes urokinase-type plasminogen activator receptor and enhances the activation of the integrin/FAK/Rac1 pathway in SMCs and macrophages *(6, 8)*. The concentrations of sLR11 in arteries increased 2 weeks after endothelial injury in rats *(8)*, and the neutralization of sLR11 activity by specific antibodies reduced the intimal thickness after cuff injury in mice *(5)*. Statins, as well as angiotensin II type 1 receptor blockers, have been reported to inhibit the migration of intimal SMCs via the downregulation of LR11 expression and to attenuate LR11 expression in the intimal SMCs of aortic arteriosclerotic plaques in hyperlipidemic rabbits *(9)*.

Circulating sLR11 can be immunologically detected in serum by use of specific antibodies against LR11 *(6)*. Circulating concentrations of LR11 were positively correlated with intimal-media thickness in dyslipidemic individuals, and the correlation was independent of other classical risk factors for atherosclerosis *(6)*. In addition, neuronal LR11 expression is characteristically reduced in mild cognitive impairment and in the brains of individuals with Alzheimer disease (AD) *(10–13)*. Single nucleotide polymorphism anal-

[1] Tsukuba Research Institute, Sekisui Medical, Ibaraki, Japan; [2] Department of Genome Research and Clinical Application, Graduate School of Medicine, Chiba University, Chiba, Japan; [3] Department of Clinical Cell Biology, Graduate School of Medicine, Chiba University, Chiba, Japan.
* Address correspondence to this author at: Tsukuba Research Institute, Sekisui Medical, 3-3-1, Koyodai, Ryugasaki, Ibaraki 301-0852, Japan. Fax +81-297-62-8635; e-mail ebinuma002@sekisui.jp.

Received March 9, 2009; accepted July 9, 2009.
Previously published online at DOI: 10.1373/clinchem.2009.127027

[4] Nonstandard abbreviations: LR11, LDL receptor relative with 11 ligand-binding repeats; SMC, smooth muscle cells; sLR11, soluble form of LR11; AD, Alzheimer disease; MAb, monoclonal antibody; CSF, cerebrospinal fluid; RAP, receptor-associated protein; PBST, PBS with Tween.

ysis of the gene for LR11 [sortilin-related receptor, L(DLR class) A repeats-containing (*SORL1*)] has been used to predict AD onset *(14, 15)*.

In this study, we produced specific monoclonal antibodies (MAbs) that bind to intact sLR11 without prior purification. Using these antibodies, we developed a novel sandwich ELISA method to quantify circulating sLR11 concentrations in both serum and cerebrospinal fluid (CSF). This technique provides a means for quantifying sLR11 to be used potentially as a marker for atherosclerosis and a predictor of AD and other neurodegenerative diseases.

Materials and Methods

BIOLOGICAL SAMPLES

Human and animal sera were purchased from Tennessee Blood Services and Cosmo Bio, respectively. Commercial human CSF samples (n = 13) were obtained from Scipac. To evaluate the normal concentration range of circulating sLR11, human serum was obtained from 87 healthy normolipidemic individuals (41 males and 46 females), who gave informed consent for participation in this study, which was approved by the Human Investigation Review Committee of the Chiba University Graduate School of Medicine.

EXTRACTION OF sLR11 WITH A RECEPTOR-ASSOCIATED PROTEIN AFFINITY RESIN

Recombinant human receptor-associated protein (RAP) was prepared as a glutathione *S*-transferase fusion protein *(16)* and applied to a glutathione-Sepharose resin (GE Healthcare), which was used to extract sLR11 from serum. Briefly, samples were incubated overnight at 4 °C at a RAP affinity resin–to–sample volume ratio of 1:20, and the resin was packed into a separation column. The column was washed with 20 mmol/L Na,K-phosphate buffer (pH 7.2) containing 150 mmol/L NaCL, and sLR11 was eluted with 50 mmol/L sodium citrate buffer (pH 5.0) containing 150 mmol/L NaCl. The sLR11 from cultured human IMR32 cells was extracted with a RAP affinity resin as described previously *(5)*.

PREPARATION OF MAb BY SYNTHETIC PEPTIDE IMMUNIZATION

Anti-LR11 MAb for use in the immunoblot analyses of human and animal sera was prepared by immunizing mice with a synthetic peptide (SMNEENMRSVITFDKG) corresponding to amino acid residues 432–447 of LR11 *(2, 17)* coupled to keyhole-limpet hemocyanin. The peptide–keyhole-limpet hemocyanin complex was emulsified with complete Freund's adjuvant (Gibco) and subcutaneously injected into BALB/c mice, 4 times at 2-week intervals. The spleen cells extracted from the immunized mice were fused with mouse myeloma cells (Sp2/0) in the presence of 50% polyethylene glycol. A single clone was selected to yield MAb A2-2–3 (IgG1,k), which reacted with both human and rabbit sLR11 in immunoblot analyses.

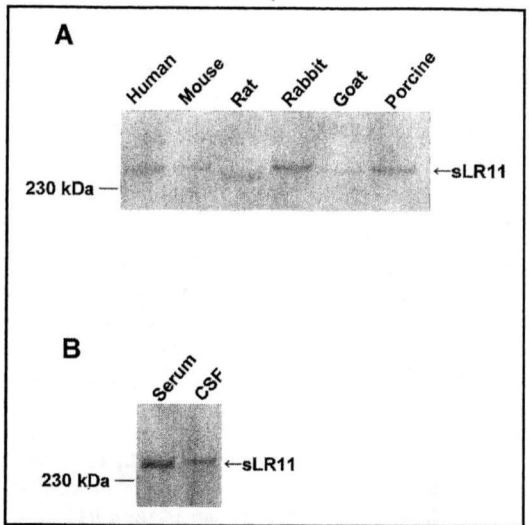

Fig. 1. Identification of sLR11 in serum and CSF.
(A), Samples (50 μL) extracted from human and animal sera by RAP affinity resin were separated by SDS-PAGE (2%–15% gradient) under reducing conditions. The sLR11 was detected by using an immunoblot assay with MAb A2-2–3. (B), Human CSF (10 μL) was separated by SDS-PAGE (2%–15% gradient) under reducing conditions, with RAP affinity-treated human serum as a control. The sLR11 protein was detected as above. A representative photo is shown. A 230-kDa marker is shown at the left in both panels.

IMMUNOBLOT ANALYSIS

Before immunoblot analysis, serum proteins were boiled in SDS-Tris buffer, with or without β-mercaptoethanol (reducing or nonreducing condition, respectively), and then separated by SDS-PAGE and transferred to a polyvinylidene difluoride membrane (Millipore). The membrane was blocked with 1% BSA in PBS containing 0.05% Tween 20 (PBST), incubated with MAb A2-2–3, reacted with horseradish peroxidase–conjugated rabbit antimouse IgG using a VECTASTAIN ABC kit (Vector Laboratories) according to the manufacturer's instructions, and subsequently stained with diaminobenzidine.

PREPARATION OF MAbs BY DNA IMMUNIZATION

Anti-LR11 MAbs for the sandwich ELISA were prepared via DNA immunization at Nosan Corporation *(18–20)*. Briefly, cDNA encoding amino acid resi-

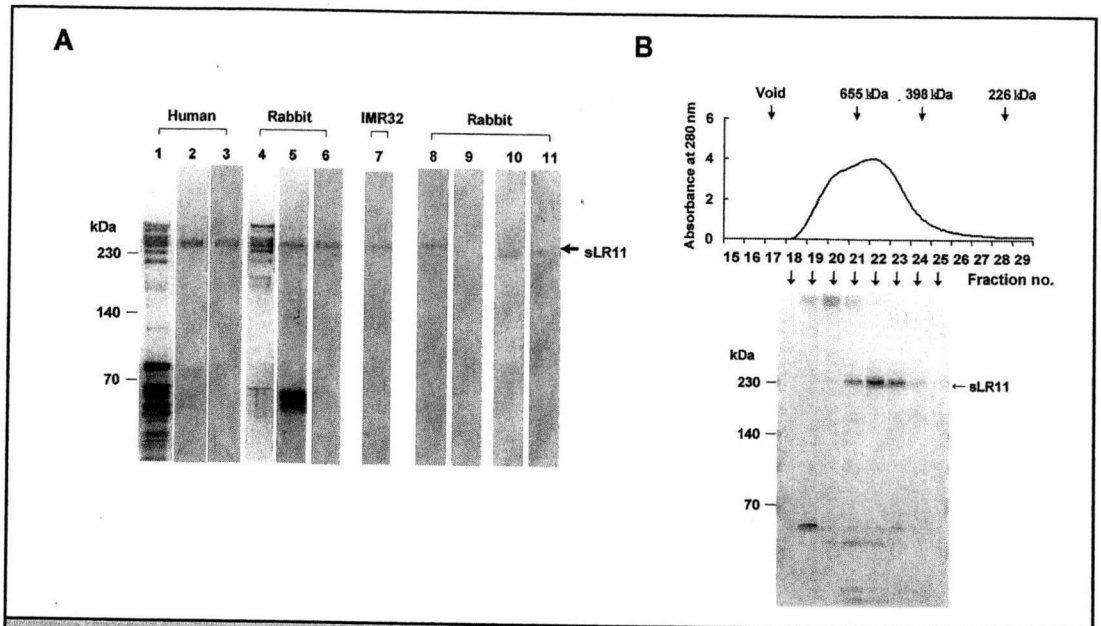

Fig. 2. Purification of sLR11 from human and rabbit serum.

(A), Samples extracted from a RAP affinity column with (lanes 2, 3, 5, 6, and 8–11) or without (lanes 1, 4, and 7) subsequent purification using an MAb-M3 affinity column were separated by SDS-PAGE (2%–15% gradient) under reducing (lanes 1–9) or nonreducing (lanes 10 and 11) conditions. Following electrophoresis, the samples were silver stained (lanes 1, 2, 4, and 5), or subjected to immunoblot analysis using MAb A2-2–3 (lanes 3, 6, and 7), R14 (lanes 8 and 10), or M3 (lanes 9 and 11). Lanes 1–3, human serum; lanes 4–6 and 8–11, rabbit serum; lane 7, human IMR32 cells. (B), Purified rabbit sLR11 protein was fractionated by gel filtration chromatography (HiLoad Superdex 200), and absorbance was monitored at 280 nm. The eluted proteins in each fraction were separated by SDS-PAGE under nonreducing conditions, and then silver stained. Markers at 230, 140, and 70 kDa are shown at the left.

dues 1000–1550 of LR11 *(2, 17)* was cloned into an expression plasmid (in-house vector, Nosan), and we immunized BALB/c mice or Wistar rats by intradermal application of DNA-coated gold particles, using a hand-held device for particle bombardment (Gene Gun, Bio-Rad). Antibody-producing cells were isolated and fused with Sp2/0 myeloma cells by use of polyethylene glycol, according to standard procedures. Five mouse and 5 rat MAbs were selected based on their reactivity with extracted rabbit sLR11, and preliminary sandwich ELISAs were performed using various combinations of these MAbs and A2-2–3. Mouse MAb M3 (IgG2a,k) and rat MAb R14 (IgG2b,k) were identified as the most sensitive for rabbit and human sLR11, respectively, and the combination of these antibodies gave the strongest reactivity against serum sLR11 in our ELISA system. Rat MAb R14 was then conjugated with sulfo-NHS-LC-biotin (Pierce), according to the manufacturer's instructions.

PURIFICATION OF sLR11 FROM HUMAN AND RABBIT SERA

The RAP affinity resin described above was used to extract sLR11 from 2.5 L of human serum or 1.0 L of rabbit serum. The eluted proteins were concentrated and applied to a HiLoad Superdex 200 gel filtration column (GE Healthcare) equilibrated with PBS. The fractions containing immunologically detected sLR11 were pooled, concentrated, and incubated overnight at room temperature with anti-LR11 MAb M3-Sepharose resin. After the resin was rinsed with PBS, immunologically bound sLR11 was eluted with 100 mmol/L sodium citrate buffer (pH 3.0). The sLR11 content was quantified by comparison with BSA standards on silver-stained gels.

SANDWICH ELISA

The wells of a polystyrene microtiter plate (Nunc) were coated with 100 μL of MAb M3 (10 mg/L in PBS) and incubated for 2 h. After extensive washing with PBST, the wells were blocked by incubation with 200 μL of

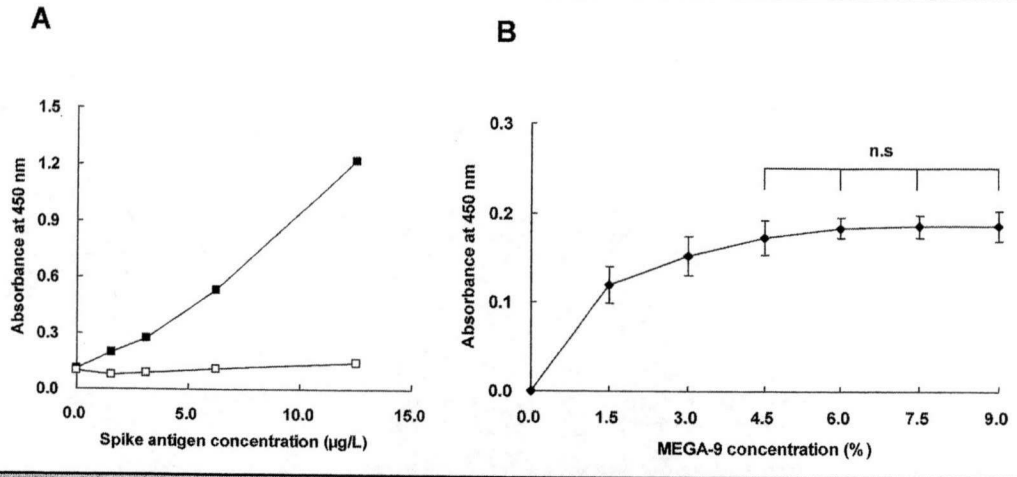

Fig. 3. The effect of MEGA-9 on ELISA measurements of sLR11 in the presence or absence of human serum.
(A), Extracted human sLR11 was measured by ELISA; sLR11 samples were diluted with PBS in the presence (□) or absence (■) of 10% human serum. (B), The sLR11 concentrations were quantified by ELISA (n = 8) in the sample buffer containing 10% human serum in the presence of various concentrations of MEGA-9. n.s., not significant.

1% BSA-PBST for 1 h. The samples (10 μL) were diluted with 100 μL of sample buffer, which consisted of 5.25% n-nonanoyl-N-methyl-d-glucamine (MEGA-9; Dojindo) and 25% heterophilic blocking reagent (Scantibodies Laboratory) in PBS. The calibration samples (0–4.0 μg/L rabbit sLR11) serially diluted in sample buffer together with the above diluted samples (100 μL) were placed into wells and then incubated for 6–16 h. After extensive washing with PBST, 100 μL of biotinylated MAb R14 was added to each well, and the plate was subsequently incubated for 4 h. After extensive washing with PBST, the LR11-MAb complex was reacted with horseradish peroxidase–conjugated streptavidin (Pierce) for 1 h. The trapped complexes were washed and incubated with 100 μL of substrate solution (tetramethyl-benzidine in citrate buffer, pH 3.65, containing hydrogen peroxide) for 30 min. The chromogenic reaction was stopped with 100 μL H_2SO_4, and the absorbance of each sample was determined at 450 nm. All steps were performed at room temperature. ELISA data (μg/L) were significantly and positively correlated with the immunoblotting data (U) previously observed following purification with RAP affinity chromatography ($r = 0.781$, $P < 0.001$, $y = 1.31\,x + 8.34$) *(6)*.

STATISTICAL ANALYSIS

Statistical analyses were performed with commercial software (Stat Flex, Ver. 5.0). The effect of sample dilution with various concentrations of MEGA-9 on the ELISA results was examined using a paired *t*-test, with $P < 0.05$ considered significant. The correlation between variables was evaluated using Pearson correlation analysis. Furthermore, sLR11 concentrations in individuals with atherosclerosis vs those in normal individuals were compared by use of box plot analysis.

Results

IDENTIFICATION OF sLR11 IN VARIOUS SERA AND HUMAN CSF

sLR11 was isolated as a 250-kDa protein from rabbit SMCs and human IMR32 cells by use of immunoblot techniques under reducing conditions and an antibody against a recombinant protein corresponding to a partial amino acid sequence of rabbit LR11 *(5)*. For comparison, sLR11 was extracted from both human and animal sera, using RAP–glutathione *S*-transferase resin. A single 250-kDa protein was detected in human serum by use of MAb A2-2–3 (Fig. 1A). The migration distance of the protein during electrophoresis was consistent with that of sLR11 from rabbit SMCs and human IMR32 cells *(5)*. A single protein band, similar in size to that obtained from human serum, was detected immunologically by MAb A2-2–3 in mouse, rat, rabbit, goat, and porcine sera. The relative intensities of the immunological signals suggested that sLR11 was most abundant in rabbit serum.

We also assessed the presence of sLR11 in human CSF (Fig. 1B), where it was identified by MAb A2-2–3 without the need for RAP extraction. Although sLR11

obtained from CSF was slightly larger than that in serum, the protein appeared as a single band at 250-kDa in both cases.

PURIFICATION OF sLR11 FROM HUMAN AND RABBIT SERA

Using DNA immunization, we established 2 MAbs, M3 and R14, against different epitopes of human sLR11; these MAbs were then used to purify intact sLR11 from serum and construct a sandwich ELISA assay. Intact sLR11 protein was first purified from human and rabbit sera using RAP affinity resin and was released from the resin with an eluting buffer, without decoupling from RAP–glutathione *S*-transferase (Fig. 2A, lanes 1 and 4). The eluted samples were treated with anti-LR11 MAb M3-Sepharose resin. Silver staining after electrophoresis indicated that the M3-reactive samples contained sLR11 as a single protein at 250 kDa as well as low molecular weight proteins, in both human and rabbit sera (lanes 2 and 5). The purified sLR11, but no other low molecular weight protein, was specifically bound to MAb A2-2–3 (lanes 3 and 6). The migration distance of sLR11 from human and rabbit sera was not different from that of sLR11 in the culture medium of IMR32 cells (lane 7). Therefore, 2-step affinity chromatography with RAP and MAb M3 can be used to specifically purify serum sLR11 as a soluble protein identical to that released from cultured cells. R14, as well as A2-2–3 and M3, showed reactivity against the purified sLR11, but did not bind any other low molecular weight protein (lanes 8–11). Notably, R14 reacted with sLR11 under both reducing and nonreducing conditions, whereas M3 reacted with sLR11 under nonreducing condition only.

Silver staining of the purified protein after gel filtration chromatography showed that the position to which purified sLR11 eluted corresponded to an estimated molecular weight >398 kDa (Fig. 2B). Notably, no other distinct protein proportional to the level of the stained sLR11 protein was detected in these fractions. The apparent molecular weight of sLR11 estimated from gel filtration was greater than that determined by use of gel electrophoresis (see Figs. 1 and 2A).

PREPARATION OF SAMPLES WITH MEGA-9 FOR SANDWICH ELISA

Sample conditions for the sandwich ELISA were determined using the above MAbs and purified samples. The absorbance level of immunologically detected sLR11 was proportional to the volume of extracted human sLR11 when diluted with PBS. However, the expected change in absorbance was not observed when samples were diluted with human serum instead of PBS (Fig. 3A). To measure sLR11 in human serum accurately, the matrix effects were mitigated by the addition of MEGA-9 detergent. The effects of MEGA-9 on absorbance recovery increased with increasing amounts

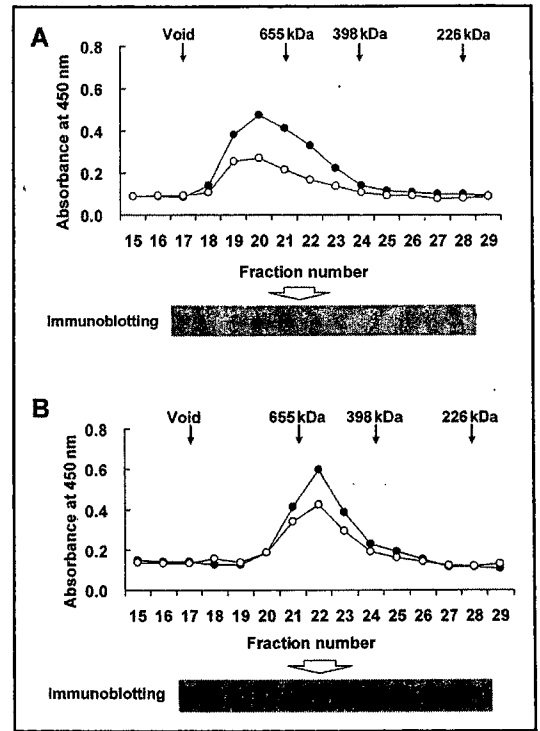

Fig. 4. Gel filtration elution profiles of sLR11 in human serum and CSF.

Human serum (A) and pooled CSF (B) samples (2 mL each) were fractionated by gel filtration chromatography (HiLoad Superdex 200), and the sLR11 concentration in each fraction was measured by ELISA in the presence (●) or absence (○) of MEGA-9. The amount of sLR11 in each fraction was also visualized by immunoblotting after extraction with the RAP affinity resin.

of MEGA-9, up to 4.5%. No significant differences were observed at higher concentrations (Fig. 3B). These results suggest that human serum contains unknown factors that interfere with sLR11 quantification, and that this interference could be diminished by the presence of MEGA-9. Therefore, samples were diluted with 5.25%, which was chosen as the middle concentration of 4.5% and 6.0%.

CHARACTERIZATION OF sLR11 IN SERUM AND CSF BY GEL FILTRATION

To assess whether ELISA can specifically detect naturally occurring sLR11, each fraction of human serum and CSF was analyzed for sLR11, following to separation by gel filtration chromatography; the results were then compared with the immunologically purified

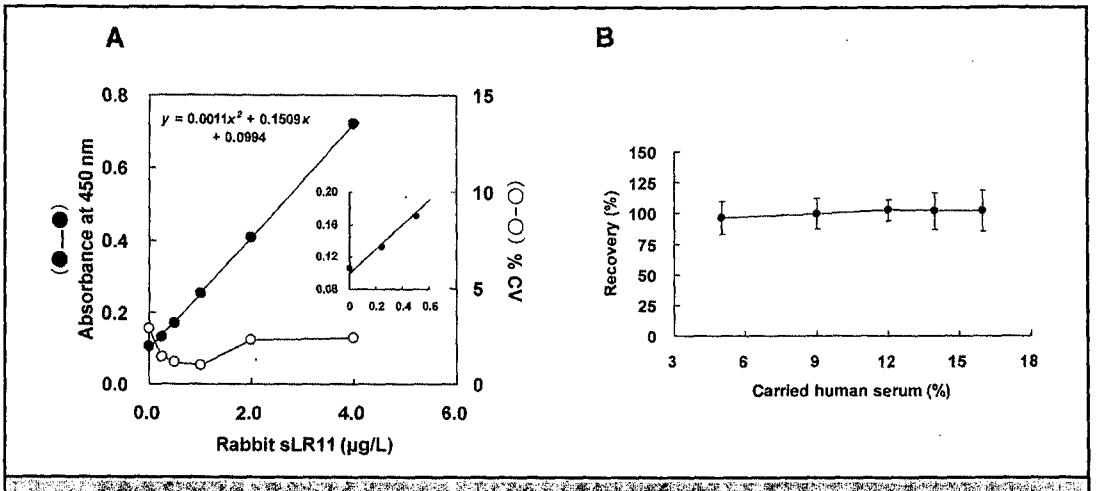

Fig. 5. Calibration curve and sample dilution test.
(A), Using the ELISA system developed in this study, we constructed a typical calibration curve (●) for sLR11 extracted from rabbit serum and the %CV of each point (○). Imprecision was assessed based on 5 replicates of the calibration curve. The insert graph is a close-up of the low-concentration area of the calibration curve. (B), Percentage recovery of purified sLR11 (2 μg/L) measured in the presence of various concentrations of human serum (5%–16%) in sample buffer. The concentration of each sample was measured using ELISA, and the percentage recoveries were calculated as a ratio of the actual-to-theoretical sLR11 concentrations.

sLR11 protein as a quantitative calibrator. The ELISA of serum and CSF samples that had been diluted with or without MEGA-9 showed abundant sLR11 in fractions with molecular weights >398 kDa (Fig. 4), similar to the results of the purified protein (see Fig. 2B). Immunoblot analyses showed that the concentration of sLR11 was proportional to the signal intensity of the gel-filtered 250-kDa proteins in both the serum and CSF samples. These results strongly suggest that this ELISA based on the immunologically purified 250-kDa sLR11 protein is also appropriate for quantifying the naturally occurring sLR11 in serum and CSF, although the gel filtration analyses suggested that the naturally occurring protein may be involved in a high molecular weight complex.

ELISA PERFORMANCE: ASSAY CHARACTERISTICS

A representative calibration curve is shown in Fig. 5A. The working range of this ELISA was 0.25–4.0 μg/L. A quadratic equation was applied to the calibration curve in the working range. The sensitivity, defined as the mean back-fit value for the lowest standard giving acceptable precision (CV = 10%), was 0.25 μg/L. With this ELISA method the lower limit of detection for sLR11 was 0.1 μg/L, which corresponds to the mean blank signal plus 3 SDs. The intraassay CVs (n = 10) were 3.0% and 3.7% at sLR11 concentrations of 7.6 μg/L in serum and 4.4 μg/L in CSF, respectively. The interassay CVs (n = 4) were 3.9% and 10.5% at sLR11 concentrations of 7.6 μg/L in serum and 4.1 μg/L in CSF, respectively. When we used samples containing 5%–16% human serum, percentage recovery ranged from 96.5% to 102.6% (Fig. 5B).

VARIATIONS OF sLR11 IN SERUM AND CSF

Measurements of sLR11 in 87 serum samples and 13 CSF samples obtained from normal individuals gave mean (SD) sLR11 concentrations of 8.7 (2.1) μg/L (range, 4.5–14.2 μg/L) and 8.5 (3.5) μg/L (range, 3.7–13.0 μg/L) in serum and CSF, respectively. We observed no significant difference in serum sLR11 concentrations between males [8.4 (1.9) μg/L, n = 41] and females [9.8 (5.8) μg/L, n = 46].

sLR11 CONCENTRATIONS IN INDIVIDUALS WITH ATHEROSCLEROSIS

To evaluate whether this ELISA method is useful for detecting variation in circulating sLR11 under pathophysiological conditions, we measured sLR11 concentrations in individuals with atherosclerosis. The sLR11 concentrations determined by immunoblotting after RAP affinity chromatography were positively correlated with the degrees of atherosclerosis in the carotid arteries of individuals with dyslipidemia *(6)*. The sLR11 concentrations in individuals with atherosclerosis were compared to those of healthy individuals (see

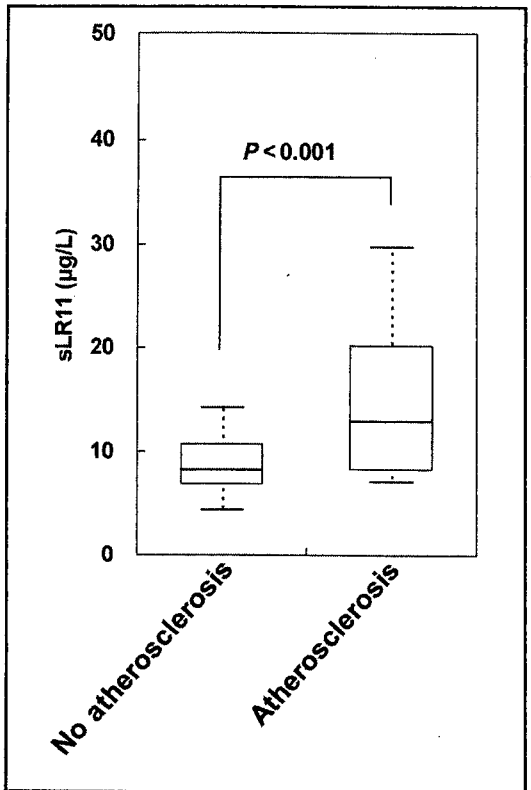

Fig. 6. Circulating sLR11 concentrations in individuals with atherosclerosis vs those in individuals without atherosclerosis.
Center horizontal lines indicate median values. Upper and lower edges of boxes, mean ± 1 SD; upper and lower bars, maximum and minimum.

previous section on variation of sLR11 in serum and CSF). The sLR11 concentrations [14.2 (6.0) µg/L] in individuals with atherosclerosis were significantly higher than those in healthy individuals (Fig. 6). The variation in circulating sLR11 concentrations in individuals with atherosclerosis was within the dynamic range of the ELISA.

Discussion

Three MAbs were established against different epitopes of human sLR11, and an ELISA method was developed for the quantitative measurement of sLR11 in serum and CSF. One of the MAbs (M3), in combination with RAP affinity extraction, enabled the purification of sLR11 from human and rabbit sera. The purified human and rabbit sLR11 was immunologically identical to sLR11 released from cultured cells, strongly suggesting that circulating sLR11 corresponds to the soluble form of membrane-bound LR11. This soluble form has been identified in the media of IMR32 and SMC cultures *(5, 6, 9)*. The combination of MAb M3 and MAb R14 yielded an ELISA that is highly specific for sLR11 in serum and CSF, without the need for prior RAP affinity extraction.

Strong matrix effects interfered with the accurate determination of sLR11 in serum by ELISA. However, these effects were diminished by pretreatment with MEGA-9 detergent (see Fig. 3). This pretreatment may dissociate complexes of sLR11 and serum components or may induce a conformational change in sLR11 such that it more efficiently interacts with the MAbs. Previous studies have shown that several serum components, including apolipoprotein E–containing lipoproteins, urokinase plasminogen activator–plasminogen activator inhibitor type 1 complex, and amyloid-β, can interact with membrane-bound LR11 *(1, 16, 21)*. The observation that MEGA-9 increased the absorbance of the isolated protein at 450 nm in gel filtration fractions obtained from both serum and CSF, and did so in proportion to the signal intensity of the sLR11 protein detected immunologically in the absence of MEGA-9 (see Fig. 4), suggests that epitope recognition by MAbs was strengthened by MEGA-9. The mechanism of MEGA-9–mediated absorbance enhancement requires further elucidation, specifically with regard to the interaction between naturally occurring sLR11 and various matrices in serum and with homomeric or heteromeric complexes under various column conditions (see Fig. 2B).

Using the established ELISA conditions, we investigated the mean sLR11 concentrations in serum and CSF. In 74% of healthy individuals, serum sLR11 concentrations were <10 µg/L. The sLR11 concentrations in the sera of individuals with atherosclerosis ranged from 6 to 30 µg/L. Therefore, the ELISA technique described here provides sufficient sensitivity for detecting circulating sLR11 concentrations in individuals with atherosclerosis and in normal populations.

Given that sLR11 is abundantly expressed in intimal SMCs *(3)* and that circulating sLR11 concentrations are positively correlated with the carotid intima-media thickness in dyslipidemic individuals *(6)*, variation in the circulating sLR11 concentration may be indicative of the condition of intimal SMCs. Metabolic disorders such as dyslipidemia and diabetes can cause pathological changes in intimal SMC function, possibly leading to accelerated progression of atherosclerosis *(22–24)*. The expression level of LR11 is drastically higher in intimal SMCs relative to that in medial SMCs *(3)*, and a large proportion of the LR11 in the cell membrane is released into the culture medium of